

# Lawrence Berkeley National Laboratory

## Recent Work

**Title**

A MULTI-WIRE PROPORTIONAL CHAMBER FOR NUCLEAR MEDICINE APPLICATIONS

**Permalink**

<https://escholarship.org/uc/item/0dz5z25r>

**Author**

Kaufman, L.

**Publication Date**

1972-04-01

A MULTI-WIRE PROPORTIONAL CHAMBER FOR  
NUCLEAR MEDICINE APPLICATIONS

L. Kaufman, V. Perez-Mendez, D. Shames,  
and G. Stoker

AEC Contract No. W-7405-eng-48



**For Reference**  
Not to be taken from this room

## **DISCLAIMER**

This document was prepared as an account of work sponsored by the United States Government. While this document is believed to contain correct information, neither the United States Government nor any agency thereof, nor the Regents of the University of California, nor any of their employees, makes any warranty, express or implied, or assumes any legal responsibility for the accuracy, completeness, or usefulness of any information, apparatus, product, or process disclosed, or represents that its use would not infringe privately owned rights. Reference herein to any specific commercial product, process, or service by its trade name, trademark, manufacturer, or otherwise, does not necessarily constitute or imply its endorsement, recommendation, or favoring by the United States Government or any agency thereof, or the Regents of the University of California. The views and opinions of authors expressed herein do not necessarily state or reflect those of the United States Government or any agency thereof or the Regents of the University of California.

0 0 0 0 3 7 0 1 1 7 5

# A MULTI-WIRE PROPORTIONAL CHAMBER FOR NUCLEAR MEDICINE APPLICATIONS

L. Kaufman\*, V. Perez-Mendez\*†, D. Shames\*, G. Stokert

\*University of California  
San Francisco, California

†Lawrence Berkeley Laboratory  
Berkeley, California

## Summary

We describe a xenon-filled multi-wire proportional chamber (MWPC) with delay-line readout of coordinates for nuclear medicine applications. This system, with an active area of  $30.5 \times 30.5 \text{ cm}^2$ , is being used to image internally administered radioisotope distributions in animals for research purposes.

## System Description

Xenon-filled MWPC's afford a simple, low cost method to detect the position of photons in the energy region below 100 keV with good accuracy and over large areas. For the purpose of imaging radio-isotope distributions, a parallel hole collimator is used to limit the photons reaching the MWPC to those which travel in a direction nearly perpendicular to it. For this work we have used three collimators: a Nuclear-Chicago High Resolution Low Energy collimator with a useful area of  $27 \times 27 \text{ cm}^2$  (NC1); a Nuclear-Chicago High Sensitivity Low Energy collimator with the same area (NC2); and a low energy collimator assembled from 2.54 cm lengths of 0.238 - cm O.D., 0.015 - cm wall, steel tubing, in a hexagonal close packed configuration, with an area of  $10 \times 12 \text{ cm}^2$  (STC). These collimators have a resolution of approximately 2 mm at the surface.

The MWPC with an active area of  $30.5 \times 30.5 \text{ cm}^2$  is identical in construction and operation to a smaller chamber described in reference 1. This chamber, filled with a 90% Xe - 10% CO<sub>2</sub> gas mixture at atmospheric pressure, has an effective mass of  $2.21 \times 10^{-2} \text{ cm}^2$  of xenon. This yields the efficiency and sensitivity (in photons/cm<sup>2</sup> for 1 roentgen of radiation reaching the chamber) responses shown in figure 1. Energy resolution is of the order of 15%.

The chamber signals obtained as described in reference 1 are first fed into timing discriminators with pulse-height selection capabilities. Signals from the discriminators are then used in a unit that provides pile-up rejection, area of interest selection and checking for the presence of both x and y pulses within a preset coincidence interval. A dual time-to-analog converter with image magnification and positioning controls is used to generate signals that are then fed to the x,y deflection plates of a Tektronix 602 display scope. A properly timed Z-unblank signal is generated and used to activate the CRT. Event dots are generated sequentially in the scope screen and integrated by a Polaroid camera left with its shutter open. Scope bandpass limits data rates to  $\sim 10^5/\text{sec}$ . On - off control of the system is performed by a scaler-timer. Figure 2 shows a schematic arrangement of the electronics. The system, mounted on a portable cart, is shown in figure 3. The weight of the chamber and collimator assembly is approximately 45 kg, and the electronics, exclusive of the high voltage power supply

and display scope, are contained in a standard NIM bin.

The system has operated for the last four months without a single failure. The chamber is refilled in four to six week periods, an operation that requires approximately 15 minutes.

## Radioisotopes

Because a MWPC operated at atmospheric pressure is useful in the energy region below 100 keV, some of the radioisotopes presently used in standard nuclear medicine work cannot be imaged by this system. Some exceptions are I-125, Hg-197, Au-195, Xe-133, and, as availability increases, I-123. Tc-99, the most commonly used radioisotope, can be imaged, but with lower efficiency and poorer resolution than in scintillation cameras. Among the rare earths we find some suitable radioactive elements such as Ce-141 comparable in cost to Xe-133. Much of the future developments will be based on a thorough examination of the potential uses of these isotopes.

Since tissue absorption of low energy photons can be significant, in fig. 4 we show transmission by various tissue thickness as a function of energy, normalizing to the transmission of the 140 keV gamma-rays of Tc-99. It can be seen that for most imaging studies, with the exception of dense organs such as the liver, the differential absorption between 60 keV and 140 keV photon is quite acceptable.

## Stationary Imaging

Fig. 5 shows transmission images of various bar patterns obtained with 22 keV and 60 keV photons. As the energy increases, the resolution, which approaches 1 mm at 22 keV, degrades to about 2 mm at 60 keV. This problem can be eliminated by operating the chamber at a higher pressure. The figure also shows the effect of lucite absorbers - interposed between the chamber and the bar pattern, but otherwise keeping the test geometry constant - on the imaging properties of 60 keV photons.

In fig. 6 we show a comparison between images obtained with the MWPC and a conventional scintillation camera. The subject is a rat injected with 400  $\mu\text{Ci}$  of I-125 albumin, which labels the blood pool. We can see the excellent resolution and scatter rejection afforded by the MWPC at this energy. Figures 7a and b show a Picker thyroid phantom loaded with 10  $\mu\text{Ci}$  of I-125 and a rabbit's kidneys labelled with 300  $\mu\text{Ci}$  of Hg-197 respectively. In fig. 8 we show a comparison of the images of a rabbit's liver and spleen labelled with 5 mCi of Tc-99 as obtained with the MWPC and a scintillation camera. At this energy the resolution of the former is clearly poorer than that of the camera.

### Dynamic Studies

Although the ultimate dead-time is limited to about 1  $\mu$ sec by the delay line, display scope response imposes a 3  $\mu$ sec dead-time on the present system. This means 5% and 30% rejection rates at data rates of  $10^6$ /min and  $6 \times 10^6$ /min respectively. Because of its speed the system is particularly suited to dynamic studies such as estimates of regional ventilatory function, and determination of hemodynamic parameters such as cardiac output. The addition of a four-area-of-interest selector, simultaneously multi-scaled by a Packard 901 Analyzer, will allow a variety of these studies to be performed with the system. As an example of this kind of work, fig. 9 shows the image and digital data obtained by perfusing a dog with 15 mCi of Xe-133. The peak count rate exceeded  $1.7 \times 10^5$ /min, with a maxima data loss of 0.85%.

### Conclusions

A reliable, low-cost imaging system for low energy gamma-rays has been obtained. In its present form the MWPC can surpass or compete favorably with conventional imaging cameras in a variety of studies. The development of radiochemicals suited for the chamber is certain to enhance the attractiveness of the device, while operation at pressures of a few atmospheres will increase its useful energy range by increasing efficiency and improving resolution.

### References

1. L. Kaufman, V. Perez-Mendez, M. Powell, and G. Stoker, "Laminographic Excitation Camera for Thyroid Imaging", to be published in the IEEE Proceedings of the 1971 Nuclear Science Symposium.
2. A MWPC with a differing readout technique is presently being used for thyroid imaging with I-125. See R. Allemand, C. Brey, T. T. Gagelin, M. Larol, CEA, pages 327-334 of "Advances in Physical and Biological Radiation Detectors", International Atomic Energy Agency, Vienna, 1971.

### Acknowledgements

This project is supported in part by funds from U. S. Public Health Service GM-01272 of the National Institute of General Medical Sciences and the U. S. Atomic Energy Commission.

We wish to thank the Nuclear-Chicago Corporation for their generous contribution of the Low Energy collimators used in this work.

0 0 0 0 3 7 0 7 7 6

### Figure Captions

- Fig. 1: Efficiency and sensitivity (in collected events per  $\text{cm}^2$  for each roentgen reaching the detector) for a MWPC of 4 cm thickness, filled with a 90% Xe - 10%  $\text{CO}_2$  gas mixture at atmospheric pressure.
- Fig. 2: Schematic arrangement of the electronics. The signals from the MWPC are amplified (A) and fed into timing and pulse-height discriminators (T and PH D). Signals from the discriminators are used to check for pile-up and the presence of both x and y pulses within a preset coincidence interval; and also to delineate an area of interest within the chamber. A dual time-to-analog converter with image size and positioning controls generates signals that are applied to the x,y deflection plates of a display CRT, while a simultaneous Z-unblank signal is used to activate the CRT. A four-areas-of-interest selector is used for multi-scaling and to enhance the display of those areas. On-off control of the system is provided by a scaler-timer.
- Fig. 3: MWPC imaging system on a portable cart.
- Fig. 4. Transmission for various tissue thicknesses compared to the transmission of 140 keV gamma-rays.
- Fig. 5: (a) 1 mm, (b) 2 mm, and (c) 4 mm bar patterns imaged with 22 keV photons, (d) 2 mm, (e) 4 mm, and (f) 10 mm bar patterns imaged with 60 keV photons. Effect of lucite absorbers interposed between the MWPC and the bar pattern on the imaging with 60 keV photons are shown for (g) none, (h) 2.54 cm, and (i) 5.08 cm of lucite.
- Fig. 6: Rat labelled with 300  $\mu\text{Ci}$  of I-125. MWPC images are shown with (a) 4,000 counts, (b) 20,000 counts, and (c) 80,000 counts. Scintillation camera image with 100,000 counts is shown in (d). This picture was taken a day later and shows radio-iodine labelling of the thyroid gland. All pictures were obtained with the NC 1 collimator.
- Fig. 7: (a) Picker thyroid phantom with 10  $\mu\text{Ci}$  of I-125, 30,000 counts (STC collimator). (b) Rabbits kidneys labelled with 300  $\mu\text{Ci}$  of Hg-197, 80,000 counts (NC 1 collimator).
- Fig. 8: Rabbits liver and spleen labelled with 5 mCi of Tc-99, 400,000 counts. (NC 1 collimator) (a) MWPC, (b) scintillation camera.
- Fig. 9: Dog's lungs perfused with 15 mCi of Xe-133. (NC 2 collimator). The respiration rate of the animal was controlled through the study. (a) 30-second interval with approximately 60,000 counts, (b) Activity in the lungs in 1-sec intervals.

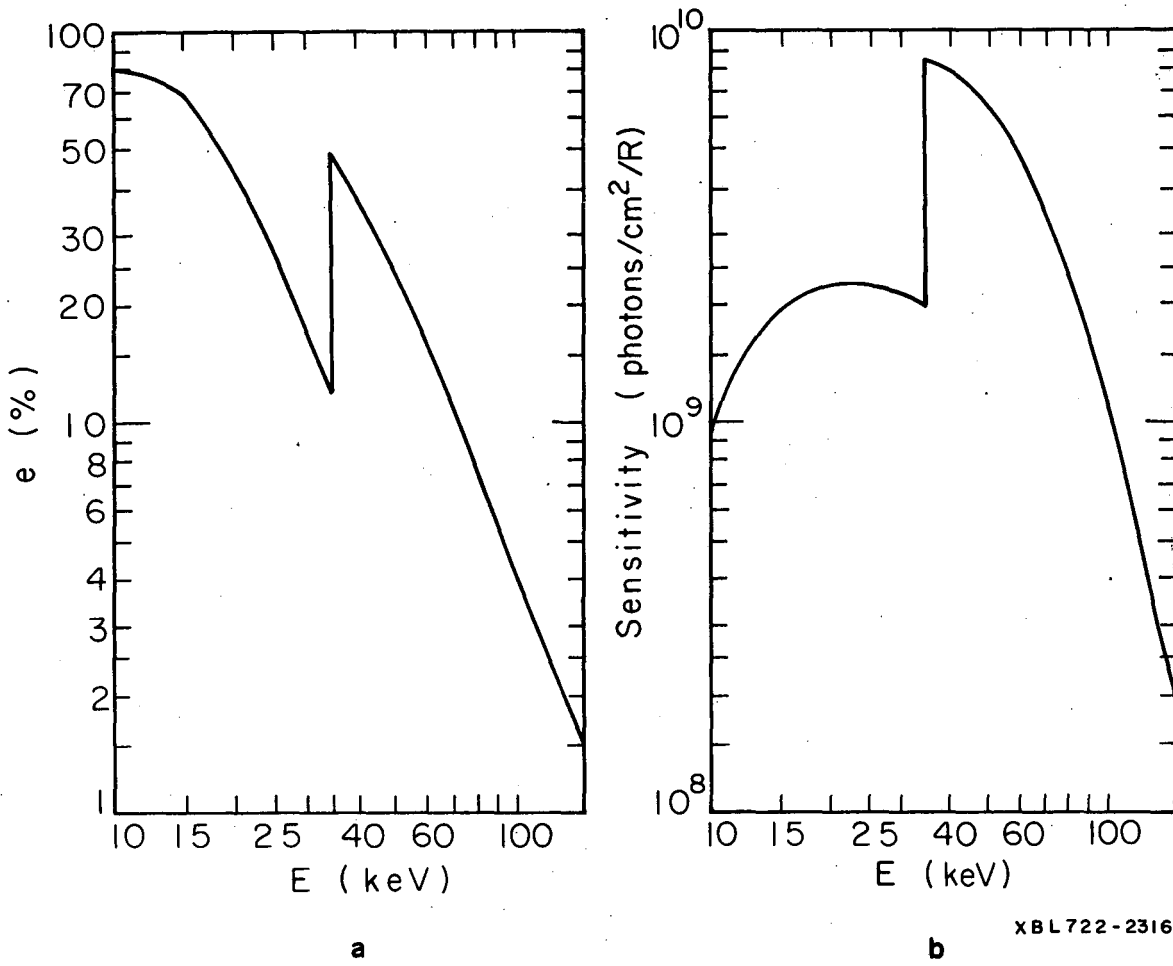


Figure 1.

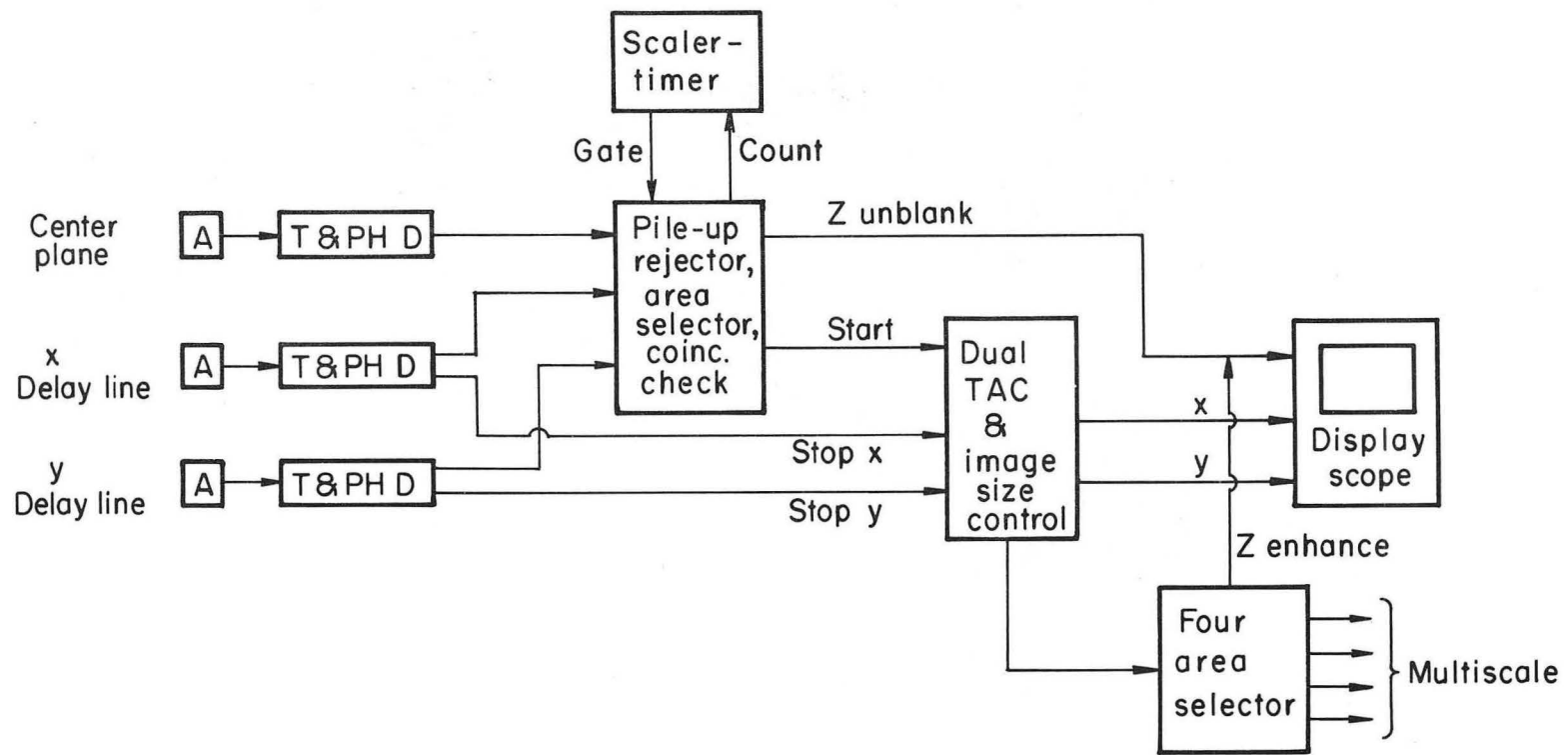
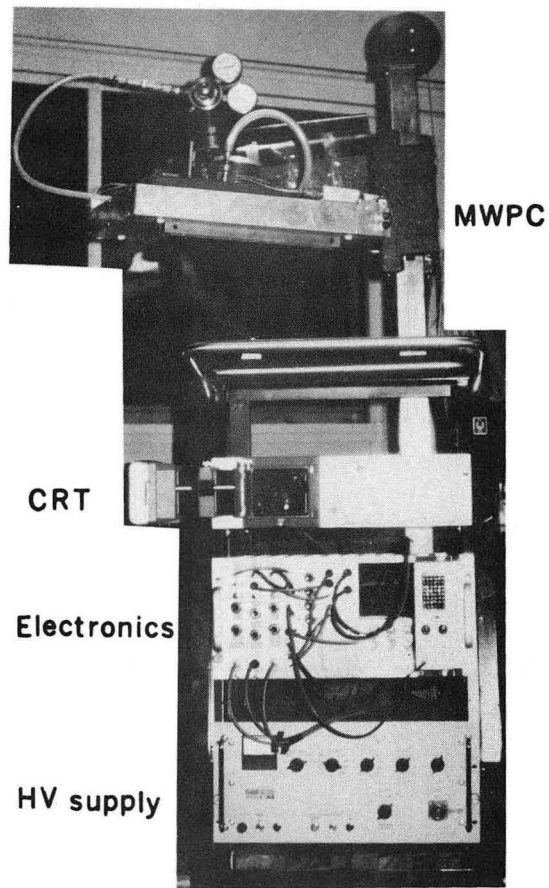


Figure 2

XBL 722-2347

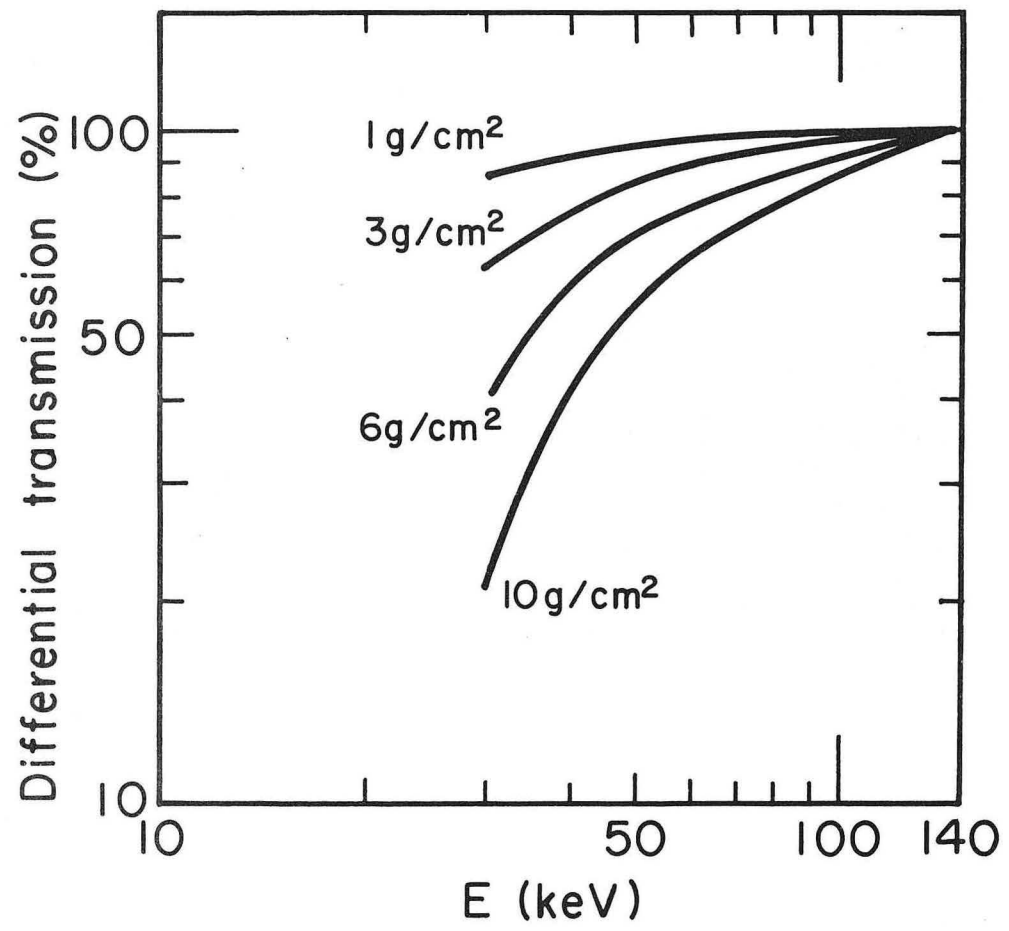
00008701111





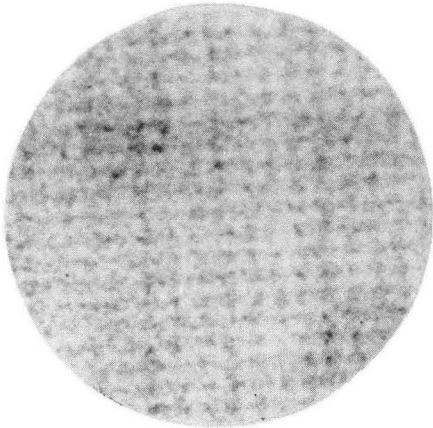
XBB-722-947

Figure 3

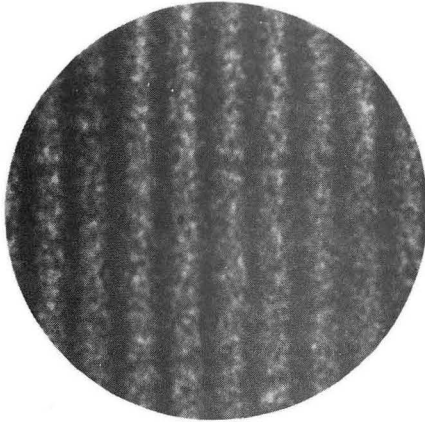


XBL 722 - 2346

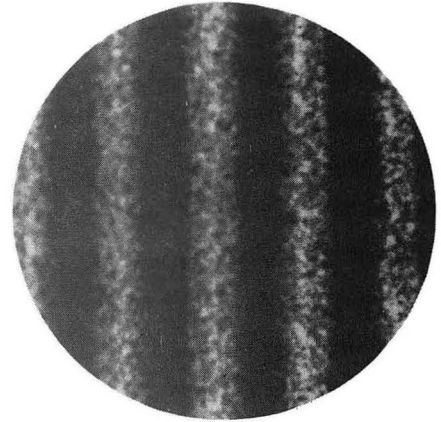
Figure 4



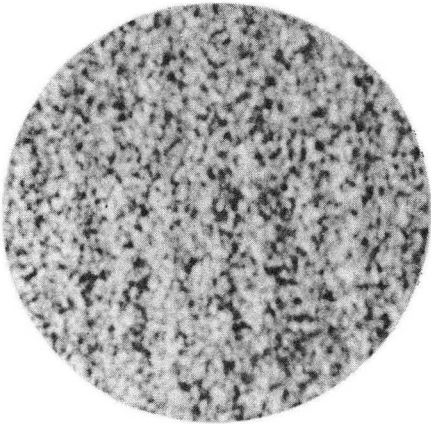
a



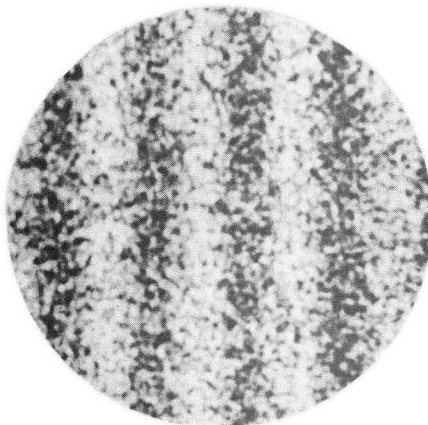
b



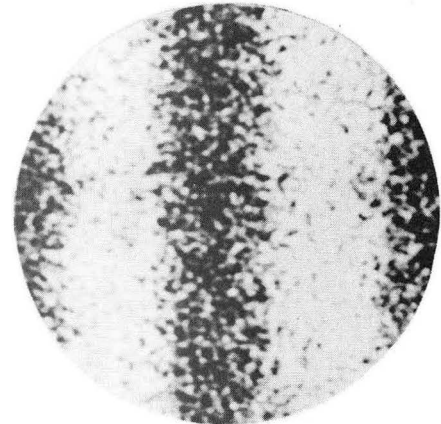
c



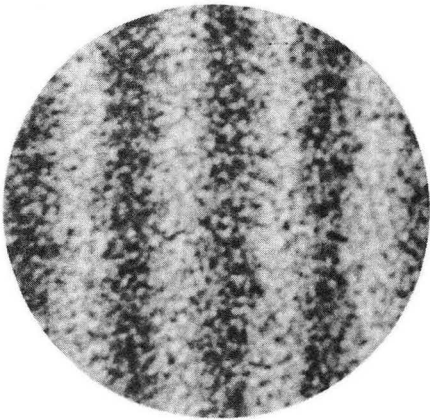
d



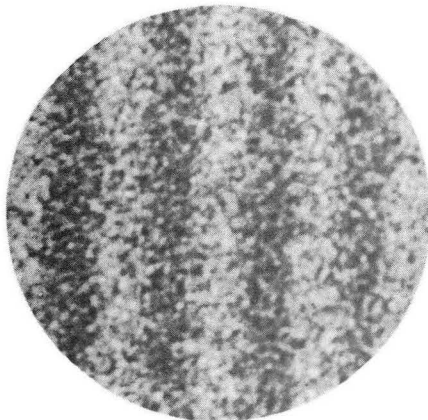
e



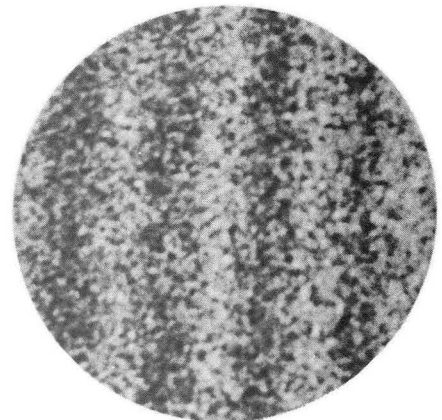
f



g

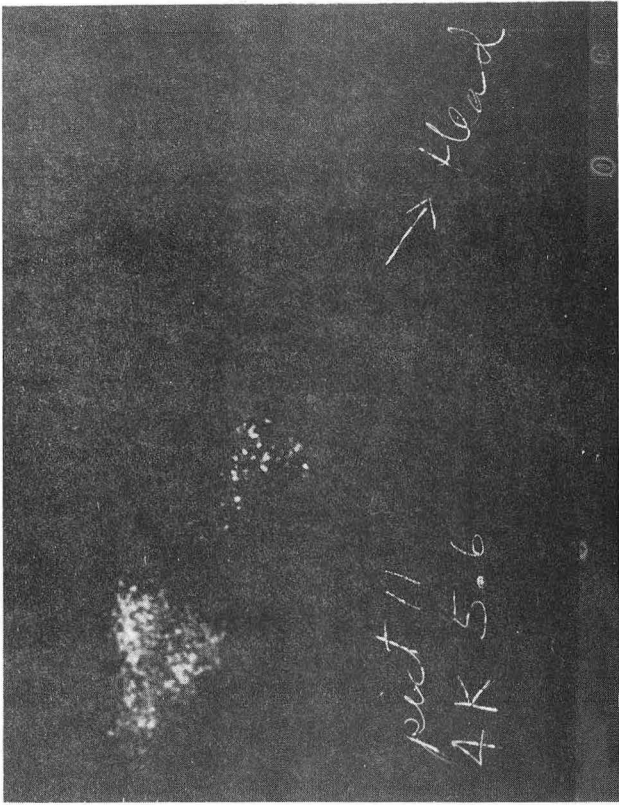


h

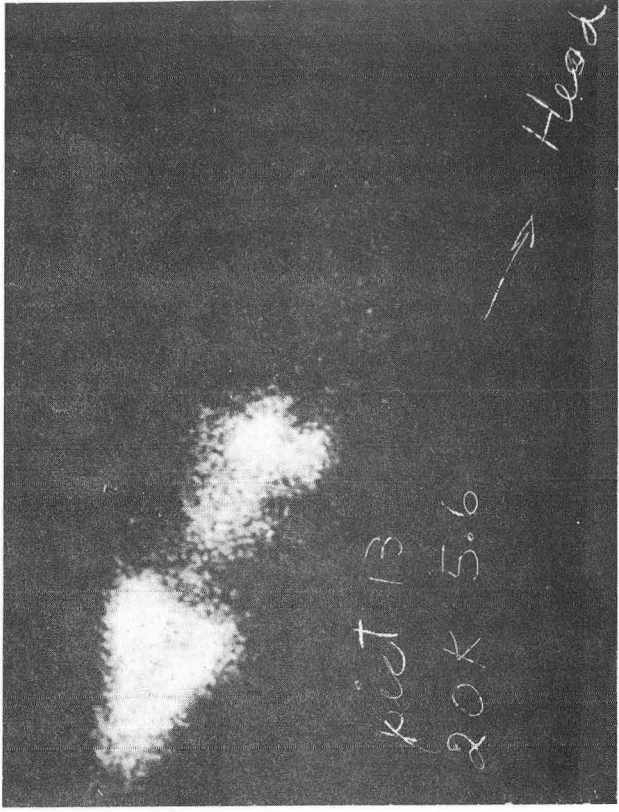


i

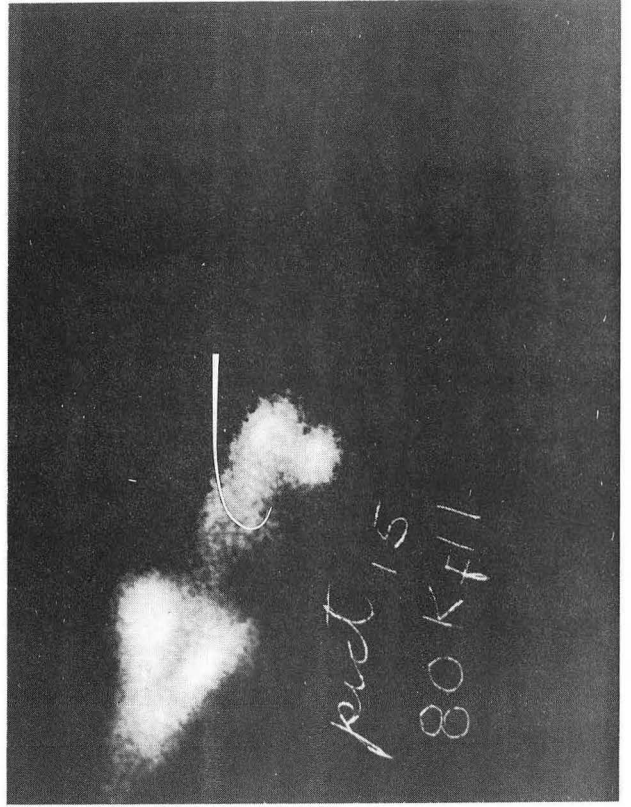
Figure 5



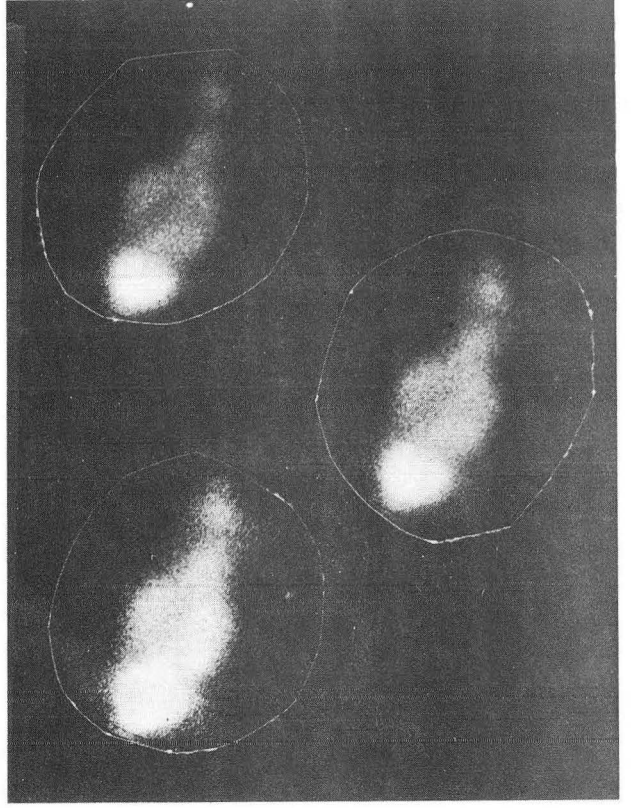
a



b

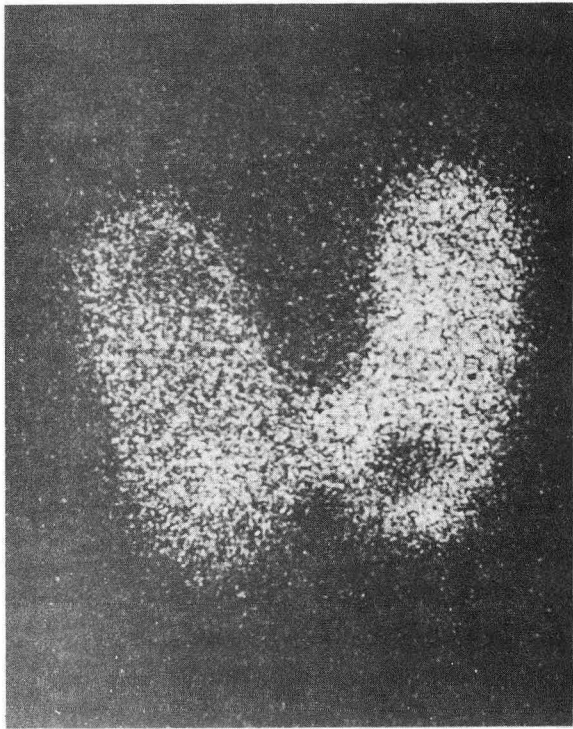


c

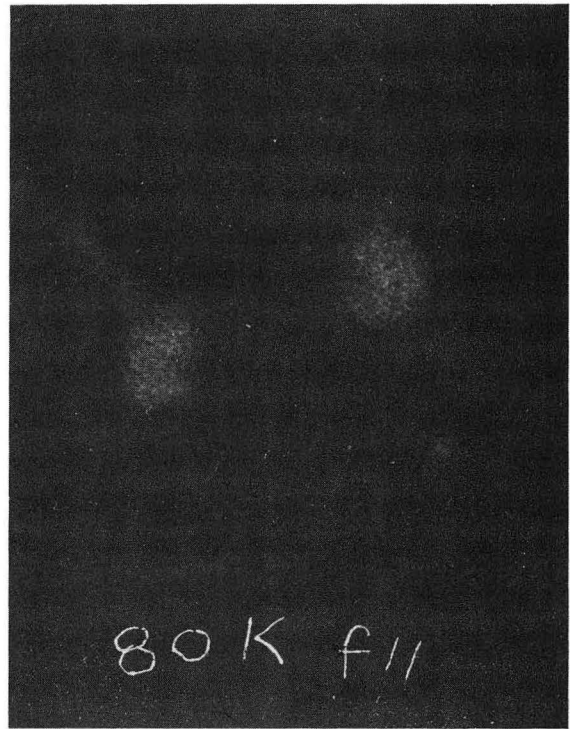


d

Figure 6



a

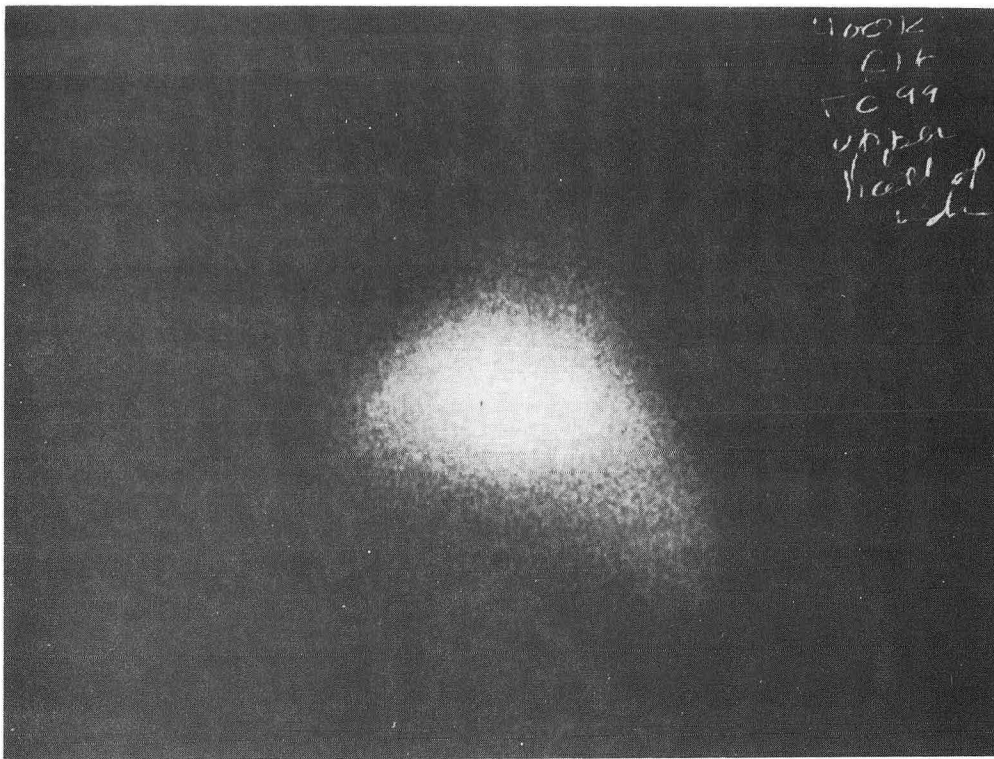


b

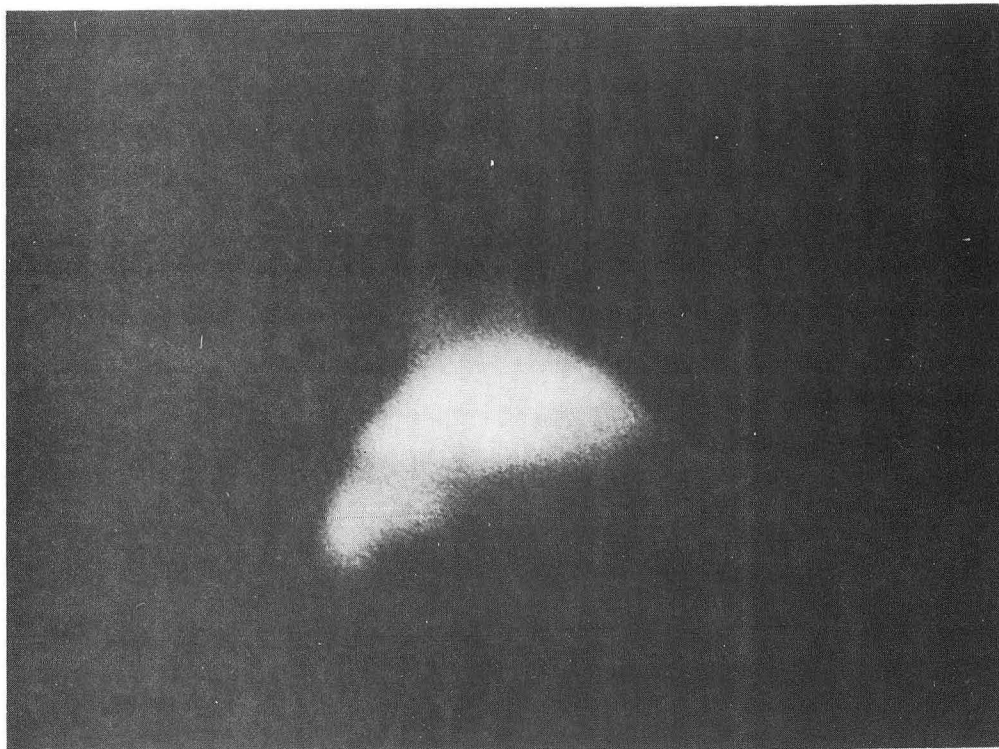
XBB 723-1373

Figure 7





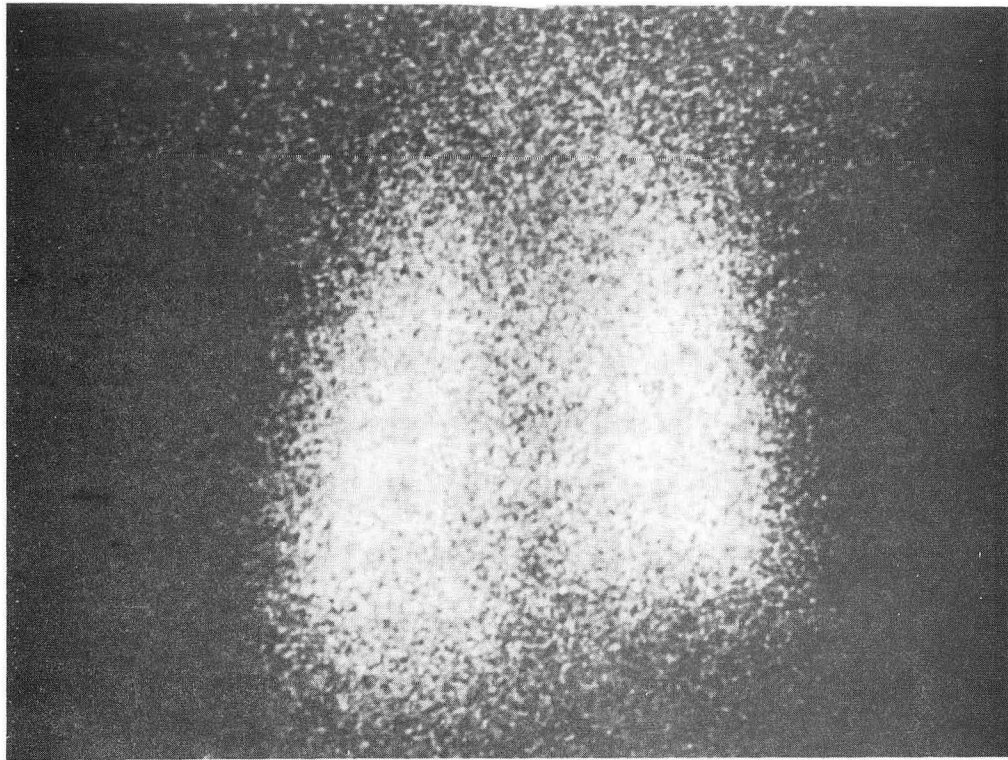
a



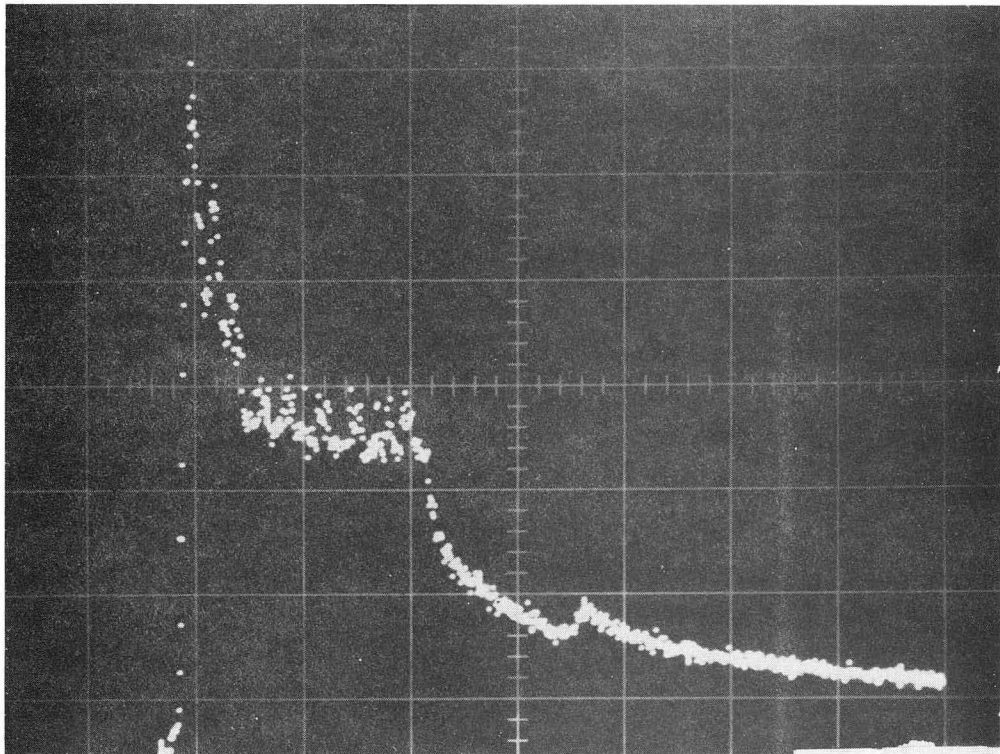
b

XBB 721-313

Figure 8



a



b

XBB 721-316

Figure 9

LEGAL NOTICE

*This report was prepared as an account of work sponsored by the United States Government. Neither the United States nor the United States Atomic Energy Commission, nor any of their employees, nor any of their contractors, subcontractors, or their employees, makes any warranty, express or implied, or assumes any legal liability or responsibility for the accuracy, completeness or usefulness of any information, apparatus, product or process disclosed, or represents that its use would not infringe privately owned rights.*



TECHNICAL INFORMATION DIVISION  
LAWRENCE BERKELEY LABORATORY  
UNIVERSITY OF CALIFORNIA  
BERKELEY, CALIFORNIA 94720